Mutual Information-based 3D Surface Matching with Applications to Face Recognition and Brain Mapping

Yalin Wang
Mathematics Department
UCLA
ylwang@math.ucla.edu

Ming-Chang Chiang
Laboratory of Neuro Imaging
UCLA School of Medicine
mcchiang@ucla.edu

Paul M. Thompson
Laboratory of Neuro Imaging
UCLA School of Medicine
thompson@loni.ucla.edu

Abstract

Face recognition and many medical imaging applications require the computation of dense correspondence vector fields that match one surface with another. In brain imaging, surface-based registration is useful for tracking brain change, and for creating statistical shape models of anatomy. Based on surface correspondences, metrics can also be designed to measure differences in facial geometry and expressions. To avoid the need for a large set of manually-defined landmarks to constrain these surface correspondences, we developed an algorithm to automate the matching of surface features. It extends the mutual information method to automatically match general 3D surfaces (including surfaces with a branching topology). We use diffeomorphic flows to optimally align the Riemann surface structures of two surfaces. First, we use holomorphic 1-forms to induce consistent conformal grids on both surfaces. High genus surfaces are mapped to a set of rectangles in the Euclidean plane, and closed genus-zero surfaces are mapped to the sphere. Next, we compute stable geometric features (mean curvature and conformal factor) and pull them back as scalar fields onto the 2D parameter domains. Mutual information is used as a cost functional to drive a fluid flow in the parameter domain that optimally aligns these surface features. A diffeomorphic surface-to-surface mapping is then recovered that matches face or anatomy in 3D. Lastly, we present a spectral method that ensures that the grids induced on the target surface remain conformal when pulled through the correspondence field. Using the chain rule, we express the gradient of the mutual information between surfaces in the conformal basis of the source surface. This finite-dimensional linear space generates all conformal reparameterizations of the surface. Illustrative experiments apply the method to face recognition problems and to the registration of brain structures, such as the hippocampus in 3D MRI scans, a key step in understanding brain shape alterations in Alzheimer's disease and schizophrenia.

1. Introduction

Many face recognition algorithms have been proposed in the last few decades [24]. Several approaches (e.g., "eigenface" methods) encode patterns of geometric and intensity variation between faces, and compute metrics to determine the degree of differences between individual faces. Related work has focused on image matching for tracking facial features in video images. However, all 2D (image-based) face recognition systems are somewhat sensitive to facial expressions and illumination conditions. 3D geometric surface matching can solve these problems and may offer better recognition performance.

Surface models are also widely used in medical imaging to assist in data visualization, nonlinear image registration, and surface-based signal processing or statistics. Surface models are often generated in computational anatomy studies to support computations, e.g. when statistically combining or comparing 3D anatomical models across subjects, or mapping functional imaging parameters onto anatomical surfaces. Often the comparison of data on two anatomical surfaces is required, and a correspondence field must be computed to register one surface nonlinearly onto the other. Multiple surfaces can be registered nonlinearly to construct a mean shape for a group of subjects, and deformation mappings can encode shape variations around the mean. This type of deformable surface registration has been used to detect developmental and disease effects on brain structures such as the corpus callosum and basal ganglia [26], the hippocampus [7], and the cortex [27]. Nonlinear matching of brain surfaces can also be used to track the progression of neurodegenerative disorders such as Alzheimer's disease [7], to measure brain growth in development [26], and to reveal directional biases in gyral pattern variability [19].

Surface registration has numerous applications, but a

direct mapping between two 3D surfaces is challenging to compute. Often, higher order correspondences must be enforced between specific anatomical points, curved landmarks, or subregions lying within the two surfaces. One common way to achieve this is to first map each of the 3D surfaces to canonical parameter spaces such as a sphere [11, 3] or a planar domain [20]. The surface correspondence problem can then be addressed by computing a flow in the parameter space of the two surfaces [26, 9], which induces a correspondence field in 3D. Finally, correspondences may be determined by using a minimum description length (MDL) principle, based on the compactness of the covariance of the resulting shape model [10]. Anatomically homologous points can then be forced to match across a dataset.

By the Riemann uniformization theorem, all surfaces can be conformally embedded in a sphere, a plane or a hyperbolic space. The resulting embeddings form special groups. Using holomorphic 1-forms and critical graphs, global conformal parameterization [15] can also be used to conformally map any high genus surface (i.e., a surface with branching topology) to a set of rectangular domains in the Euclidean plane. In this paper, we show how to use conformal parameterizations to assist in the matching of arbitrary 3D face and anatomical surfaces. Mutual information is used to drive a diffeomorphic fluid flow that is adjusted to find appropriate surface correspondences in the parameter domain. In this study, we chose the mean curvature and the conformal factor of the surfaces as the differetial geometric features to be aligned, as these are intrinsic and stable. These choices are purely illustrative. In fact, any scalar fields defined on the surfaces could be matched, e.g. cortical thickness maps, or even functional imaging signals or metabolic data. Since conformal mapping and fluid registration techniques generate diffeomorphic mappings, the 3D shape correspondence established by composing these mappings is also diffeomorphic (i.e., provides smooth one-to-one correspondences).

We also present a spectral approach for ensuring that the grid induced on the target surface by the correspondence field, remains conformal. Grid orthogonality is advantageous for accurate numerical discretization of PDEs or for signal processing on the resulting surface meshes. For high genus surfaces, the global conformal parameterization is not unique and all the conformal parameterizations form a linear space. The degrees of freedom in this space of conformal grids are tuned to maximize the mutual information energy of features between the two surfaces. Because the conformal structure is intrinsic and the conformal parameterization continuously depends on the Riemannian metric on the surface, our method is also stable and computationally efficient.

1.1. Previous Work

Some researchers [17, 21] incorporate 3D model in face recognition research. Bronstein et al. [5] propose a 3D face recognition approach based on geometric invariants to isometric deformations. Several variational or PDE-based methods have been proposed for matching surfaces. Surfaces may be represented by parametric meshes [11], level sets, or both representations [20]. Angenent et al. [2, 1] represent the Laplace-Beltrami operator as a linear system and implement a finite element approximation for parameterizing brain/colon surfaces via conformal mapping. Gu et al. [13] found a unique conformal mapping between any two genus zero manifolds by minimizing the harmonic energy of the map. Gu and Vemuri [12] also matched 3D shapes by first conformally mapping them to a canonical domain and aligning their 2D representations over the class of diffeomorphisms. They demonstrated their algorithm on genus zero closed surfaces.

The mutual information (MI) method [29, 28] measures the statistical dependence of the voxel intensities between two images. This measure of agreement can be used to tune the parameters of a registration transform such that MI is maximal when the two images are optimally aligned. The MI method has been successful for rigid [30] and non-rigid [22, 25] image registration. Here, we generalize it to match 3D surfaces. For MI to work, a monotonic mapping in grayscales between images is not required, so images from different modalities can be registered [18]. Hermosillo et al. [16] adopted linear elasticity theory to regularize the variational maximization of MI. D'Agostino et al. [8] extended this approach to a viscous fluid scheme allowing large local deformations, while maintaining smooth, one-to-one topology [6].

1.2. Basic Idea

Suppose S_1 is an oriented surface. The map from S_1 to a local coordinate (x_1, x_2) plane is a *conformal map* when the first fundamental form satisfies: $ds^2 = \lambda(u,v)^2(du^2 + dv^2)$. Here $\lambda(u,v)$ is called the *conformal factor*, a function that scales the metric at each point (u,v). We say (x_1, x_2) is a conformal coordinate of X_1. Locally, each surface patch is covered by a conformal coordinate chart. For high genus surfaces, the local conformal parameterization can be extended to cover the whole surface. By the Riemann-Roch theorem and the circle-valued Morse theorem, a high genus surface ($g \geq 1$) can be completely covered by a set of non-overlapping segments. Each segment can be conformally mapped to a rectangle. With the Gauss and Codazzi equations, one can prove that a closed surface $r(u,v)$ in R^3 with conformal parameter (u,v) is uniquely determined by its conformal factor $\lambda(u,v)$ and its mean cur-

vature $H(u,v)$, up to a rigid motion. We call a tuple of (u,v) and $H(u,v)$ a *conformal representation* of the surface $r(u,v)$. We can solve the surface registration problem by computing intrinsic geometric features from the conformal mesh, and aligning them in the parameterization domain. To align these scalar fields, we use a fluid registration technique in the parameter domain that is driven by mutual information. With conformal mapping, we essentially convert the surface registration problem into an image registration problem, for which MI methods are especially advantageous. Finally, by invoking the surface partitioning technique induced by holomorphic 1-forms, our surface-based mutual information method works on general surfaces with arbitrary topologies.

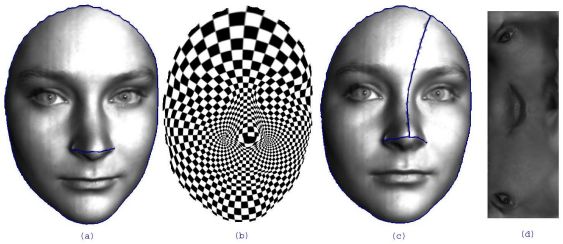

Figure 1. Illustrates surface conformal structure. (a) shows the cut we introduce on a face surface. The face becomes an open boundary genus one surface. (b) shows a global conformal parameterization of the surface. (c) shows the horizontal trajectory. (d) shows the rectangle to which the face surface is conformally mapped.

2. Theoretical Background

2.1. Global Conformal Parameterization

Suppose M_1, M_2 are two surfaces. Locally they can be represented as $r_1(x^1,x^2)$, $r_2(x^1,x^2)$, where (x^1,x^2) are their local coordinates, and $r_1, r_2 : R^2 \to R^3$ are vector-valued functions. The first fundamental form of M_1 is $ds_1^2 = \sum_{ij} g_{ij} dx^i dx^j$, where $g_{ij} = \frac{\partial r_1}{\partial x^i} \cdot \frac{\partial r_1}{\partial x^j}, i,j = 1,2$. Similarly, the first fundamental form of M_2 is defined in the same way: $ds_2^2 = \sum_{ij} \tilde{g}_{ij} dx^i dx^j$. Define a mapping $f : M_1 \to M_2$ between two surfaces. Using local coordinates, f can be represented as $f : R^2 \to R^2$, $f = (f^1(x^1,x^2), f^2(x^1,x^2))$. Then any tangent vector (dx^1, dx^2) on M_1 will be mapped to a tangent vector df on M_2,

$$\begin{pmatrix} df^1 \\ df^2 \end{pmatrix} = \begin{pmatrix} \frac{\partial f^1}{\partial x^1} & \frac{\partial f^1}{\partial x^2} \\ \frac{\partial f^2}{\partial x^1} & \frac{\partial f^2}{\partial x^2} \end{pmatrix} \begin{pmatrix} dx^1 \\ dx^2 \end{pmatrix} \quad (1)$$

The length of df is $\sum_{m,n} \tilde{g}_{mn} df^m df^n$. We use the length of df to define the length of (dx^1, dx^2). Namely, we define a new metric for M_1 which is induced by the mapping f and the metric on M_2. We call this metric *the pull-back metric*, and denote it by $f^* ds_2^2$. Replacing df^m in the above equation by (1), we get the analytic formula for the pull-back metric,

$$f^* ds_2^2 = \sum_{mn} \Big(\sum_{ij} \tilde{g}_{ij}(f(x^1,x^2)) \frac{\partial f^m}{\partial x_i} \frac{\partial f^n}{\partial x_j} \Big) dx^m dx^n. \quad (2)$$

We call f a *conformal mapping*, if there exists a positive scalar function $\lambda(x^1,x^2)$, such that $f^* ds_2^2 = \lambda(x^1,x^2) ds_1^2$. where $\lambda(x^1,x^2)$ is called the *conformal factor*.

Intuitively, all the angles on M_1 are preserved on M_2. Figure 1 shows a conformal mapping example. Figure 1 shows a face surface. We introduce a cut on the nose (a) and change it to a genus one surface. We illustrate the conformal parameterization via the texture mapping of a checkerboard in (b). By tracing horizontal trajectory (c), we conformally map it to a square as in (d) and get its conformal parameterization.

An *atlas* is a collection of consistent coordinate charts on a manifold, where transition functions between overlapping coordinate charts are smooth.

We treat R^2 as isomorphic to the complex plane, where the point (u,v) is equivalent to $z = u + iv$, and $(u,-v)$ is equivalent to $\bar{z} = u - iv$. Let S be a surface in $\mathbb{R}^3$ with an atlas $\{(U_\alpha, z_\alpha)\}$, where (U_α, z_α) is a chart, and $z_\alpha : U_\alpha \to \mathbb{C}$ maps an open set $U_\alpha \subset S$ to the complex plane $\mathbb{C}$.

An atlas is called *conformal* if **(1).** each chart (U_α, z_α) is a conformal chart. Namely, on each chart, the first fundamental form can be formulated as $ds^2 = \lambda(z_\alpha)^2 dz_\alpha d\bar{z_\alpha}$; **(2).** the transition maps $z_\beta \circ z_\alpha^{-1} : z_\alpha(U_\alpha \cap U_\beta) \to z_\beta(U_\alpha \cap U_\beta)$ are holomorphic.

A chart is compatible with a given conformal atlas if adding it to the atlas again yields a conformal atlas. A *conformal structure* (*Riemann surface structure*) is obtained by adding all compatible charts to a conformal atlas. A *Riemann surface* is a surface with a conformal structure.

One coordinate chart in the conformal structure introduces a *conformal parameterization* between a surface patch and the image plane. The conformal parameterization is angle-preserving and intrinsic to the geometry, and is independent of the resolution and triangulation.

Locally, a surface patch is covered by a conformal coordinate chart. For high genus surfaces, the local conformal parameterization can be extended to cover the whole surface except at several points. These exceptional points are called *zero points*. By the Riemann-Roch theorem, there are $2g-2$ zero points on a global conformal structure of a genus g closed surface. By the circle-valued Morse theorem, the iso-parametric curves through the zero points segment the whole segment the whole surface to patches, where each patch is either a topological disk, or a cylinder. The segmentation is determined by the conformal structure of the

surface and the choice of the global conformal parameterization.

Figure 2 shows an example of the conformal parameterization of a dog surface model. We introduce 3 cuts on the surface and change it to a genus 2 surface. The computed conformal structure is shown in (a). (b) shows a partition of the dog surface, where each segment is labeled by a unique color. (d) shows the parameterization domain. Each rectangle is the image, in the parameterization domain, of a surface component in (c).

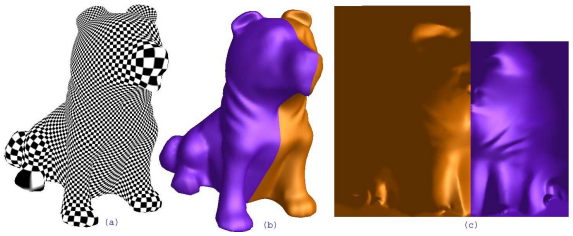

Figure 2. Illustrates conformal parameterization for a high genus surface. (a) shows the conformal structure for a model of a dog. After introducing cuts between both ears and on the bottom, we turn the dog model to an open boundary genus 2 surface. (b) shows a partition of this surface, with a unique color labeling each part. (c) shows the parameterization domain. Each surface component in (b) is conformally mapped to a rectangle in (c). The color scheme shows the association between elements in (b) and (c).

2.2. Optimal Global Conformal Parameterization

Given a Riemann surface S with a conformal atlas $\{(U_\alpha, z_\alpha)\}$, a holomorphic 1-form ω is defined by a family $\{(U_\alpha, z_\alpha, \omega_\alpha)\}$, such that **(1).** $\omega_\alpha = f_\alpha(z_\alpha)dz_\alpha$, where f_α is holomorphic on U_α, and **(2).** if $z_\alpha = \phi_{\alpha\beta}(z_\beta)$ is the coordinate transformation on $U_\alpha \cap U_\beta (\neq \emptyset)$, then $f_\alpha(z_\alpha)\frac{dz_\alpha}{dz_\beta} = f_\beta(z_\beta)$, i.e., the local representation of the differential form ω satisfies the chain rule.

For a Riemann surface S with genus $g > 0$, all holomorphic 1-forms on S form a complex g-dimensional vector space ($2g$ real dimensions), denoted by $\Omega^1(S)$. The conformal structure of a higher genus surface can always be represented in terms of a holomorphic one-form basis, which is a set of $2g$ functions $\omega_i : K_1 \to R^2, i = 1, 2 \cdots, 2g$. Any holomorphic one-form ω is a linear combination of these functions. The quality of a global conformal parameterization for a high genus surface is fundamentally determined by the choice of the holomorphic 1-form.

Figure 3 shows two different conformal parameterizations of a lateral ventricle surface of a HIV/AIDS patient subject. (a) shows a uniform parameterization result and (b) shows a nonuniform parameterization result. Note that although both of these are conformal, one has greater area distortion than the other.

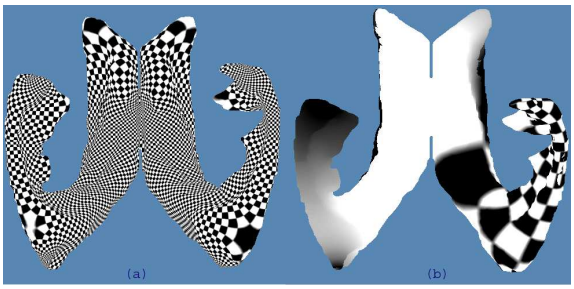

Figure 3. Shows a uniform (left panel) and a non-uniform (right panel) global conformal parameterization for the same surface, the lateral ventricles of the human brain.

2.3. Conformal Representation of a General Surface

For a general surface S, we can compute conformal coordinates (u, v) to parameterize S. Based on these coordinates, one can derive scalar fields including the conformal factor, $\lambda(u, v)$, and mean curvature, $H(u, v)$, of the surface position vector $S(u, v)$:

$$\frac{\partial S}{\partial u} \times \frac{\partial S}{\partial v} = \lambda(u, v)\vec{n}(u, v) \tag{3}$$

$$H(u, v) = |\frac{1}{\lambda^2(u, v)}(\frac{\partial^2}{\partial u^2} + \frac{\partial^2}{\partial v^2})\vec{r}(u, v)| \tag{4}$$

We can regard the tuple (λ, H) as the conformal representation of $S(u, v)$. We have the following theorem [14].

Theorem: *A closed surface $S(u, v)$ in R^3 with conformal parameter (u, v) is uniquely determined by its conformal factor $\lambda(u, v)$ and its mean curvature $H(u, v)$ up to rigid motions. A simply connected surface $r(u, v)$ with a boundary in R^3 and conformal parameter (u, v) is determined by its conformal factor $\lambda(u, v)$ and its mean curvature $H(u, v)$ and the boundary position.*

Clearly, various fields of scalars or tuples could be used to represent surfaces in the parameter domain. Because the conformal structure is intrinsic and independent of the data resolution and triangulation, we use the conformal representation, $\lambda(u, v)$ and $H(u, v)$, represent the 3D surfaces. This representation is stable and computationally efficient. Figure 4 illustrates computed conformal factor and mean curvature indexed by color on a hippocampal surface.

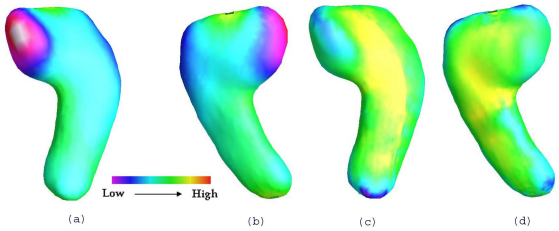

Figure 4. Illustrates the computed conformal factor and mean curvature on a hippocampus surface. On the left are two views of the hippocampal surface, colored according to the conformal factor. The right two are colored by mean curvature.

2.4. Mutual Information for Surface Registration

We now describe the mutual information functional used to drive the scalar fields $\lambda(u,v)$ and $H(u,v)$ into correspondence, effectively using the equivalent of a 2D image registration in the surface parameter space (i.e., in conformal coordinates). Let I_1 and I_2 be the target and the deforming template images respectively, and $I_1, I_2 : R^2 \rightarrow R$. Let $\Omega \subset R^2$ be the common parameter domain of both surfaces (if both are rectangular domains, the target parameter domain can first be matched to the source parameter domain using a 2D diagonal matrix). Also, let u be a deformation vector field on Ω. The MI of the scalar fields (treated as 2D images) between the two surfaces is defined by

$$I(u) = \int_{R^2} p_u(i_1, i_2) log \frac{p_u(i_1, i_2)}{p(i_1) p_u(i_2)} di_1 di_2 \quad (5)$$

where $p(i_1) = P(I_1(x) = i_1), p_u(i_2) = P(I_2(x-u) = i_2)$ and $p_u(i_1, i_2) = P(I_1(x)) = i_1$ and $I_2(x-u) = i_2$.

We adopted the framework of D'Agostino et al. [8] to maximize MI with viscous fluid regularization. Briefly, the deforming template image was treated as embedded in a compressible viscous fluid governed by Navier-Stokes equation for conservation of momentum [6], simplified to a linear PDE:

$$Lv = \mu \nabla^2 v + (\lambda + \mu) \vec{\nabla}(\vec{\nabla} \cdot v) + F(x,u) = 0 \quad (6)$$

Here v is the deformation velocity, and μ and λ are the viscosity constants. Following the derivations in [8], we take the first variation of $I(u)$ with respect to u, and use the Parzen window method [23] to estimate the joint probability density function (pdf) $p_u(i_1, i_2)$. The driving force $F(x,u)$ that registers features in the 2D surface parameter space is given by

$$F(x,u) = \frac{1}{A} [L_u(i_1, i_2) * \frac{\partial \Psi_h}{\partial i_2}](I_v(x), I_2(x-u)) \nabla I_2(x-u) \quad (7)$$

where A is the area of the parameter domain $\Omega, L_u(i_1, i_2) = 1 + log \frac{p_u(i_1, i_2)}{p(i_1) p_u(i_2)}$, $\Psi_h(i_1, i_2) = \phi_h(i_1)\phi_h(i_2) = (\sqrt{2\pi}h)^{-1} \cdot exp(-i_1^2/2h^2) \cdot (\sqrt{2\pi}h)^{-1} \cdot exp(-i_2^2/2h^2)$ as the Parzen kernel, and "$*$" denotes convolution.

3. The Surface Mutual Information Method for an Arbitrary Genus Surface

Next, suppose we want to match two high genus surfaces (i.e., surfaces with the same branching topology). To apply our surface mutual information method piecewise, we first compute the conformal representations of the two surfaces based on a global conformal parameterization. Mutual information driven flows are then applied to align the computed conformal representations, while enforcing constraints to guarantee continuity of the vector-valued flow at the patch boundaries. When the chain rule is used, we can further optimize the mutual information matching results by optimizing the underlying global conformal parameterization.

Let S_1 and S_2 be two surfaces we want to match and the conformal parameterization of S_1 is τ_1, conformal parameterization for S_2 is τ_2, $\tau_1(S_1)$ and $\tau_2(S_2)$ are rectangles in R^2. Instead of finding the mapping ϕ from S_1 to S_2 directly, we can use mutual information method to find a diffeomorphism $\tau : D_1 \rightarrow D_2$, such that the diagram below commutes: $\tau_2^{-1} \circ \tau \circ \tau_1 = \phi$. Then the map ϕ can be obtained by the following commutative diagram,

$$\begin{array}{ccc} S_1 & \xrightarrow{\phi} & S_2 \\ {\scriptstyle ,\tau_1}\downarrow & & \downarrow{\scriptstyle \tau_2} \\ R^2 & \xrightarrow{\tilde{\tau}} & R^2 \end{array} \quad (8)$$

$\phi = \tau_1 \circ \tau \circ \tau_2^{-1}$. Because τ_1, τ and τ_2 are all diffeomorphisms, ϕ is also a diffeomorphism.

3.1. Mutual Information Contained in Maps between High Genus Surfaces

A global conformal parameterization for a high genus surface can be obtained by integrating a holomorphic one-form ω. Suppose $\{\omega_i, i = 1, 2, \cdots, 2g\}$ is a holomorphic 1-form basis, where an arbitrary holomorphic 1-form has the formula $\omega = \sum_{i=1}^{2g} \lambda_i \omega_i$. Assuming the target surface's parameterization is fixed, the mutual information energy between it and the source surface's parameterization is denoted by $E(\omega)$, which is a function of the linear combination of coefficients λ_i. The necessary condition for the optimal holomorphic 1-form is straightforward, $\frac{\partial E}{\partial \lambda_i} = 0, i = 1, 2, \cdots, 2g$. If the Hessian matrix $(\frac{\partial^2 E}{\partial \lambda_i \partial \lambda_j})$ is positive definite, then E will reach the minimum. If the Hessian matrix is negative definite, E will be maximized.

Our surface mutual information method depends on the selection of holomorphic 1-form ω. To get an optimal surface mutual information matching results, we need find the optimal holomorphic 1-form for mutual information metric. Suppose a holomorphic function $\omega = \sum_{i=1}^{2g} \lambda_i \omega_i$, our goal is to find a set of coefficients $\lambda_i, i = 1, ..., 2g$ that maximize the mutual information energy, E_{MI}. We can solve this optimization problem numerically as follows:

$$dE_{MI} = (\frac{dE_{MI}}{du}, \frac{dE_{MI}}{dv}) \begin{pmatrix} \frac{du}{d\lambda_1} & \frac{du}{d\lambda_2} & \cdots & \frac{du}{d\lambda_{2g}} \\ \frac{dv}{d\lambda_1} & \frac{dv}{d\lambda_2} & \cdots & \frac{dv}{d\lambda_{2g}} \end{pmatrix} \begin{pmatrix} d\lambda_1 \\ d\lambda_2 \\ \cdots \\ d\lambda_{2g} \end{pmatrix} \quad (9)$$

where (u, v) is the conformal coordinate.

Once we compute $\frac{dE_{MI}}{d\lambda_i}, i = 1, 2, ..., 2g$, we can use steepest descent to optimize the resulting mutual information. A complete description of the surface mutual information method follows.

Algorithm 1 *Surface Mutual Information Method (for surfaces of arbitrary genus)*

Input (mesh M^1 and M^2,step length δt, energy difference threshold δE),

Output($t : M^1 \rightarrow M^2$) where t minimizes the surface mutual information energy.

1. *Compute global conformal parameterization of two surfaces, $\omega^j = \sum_{i=1}^{2g} s_i \omega_i, j = 1, 2; i = 1, 2, ..., 2g$, where g is the surface genus number of two surfaces M^1 and M^2, and $s_i^j, j = 1, 2, i = 1, 2, ..., 2g$ are the coefficients of a linear combination of holomorphic function basis elements. The steps include computing the homology basis, cohomology basis, harmonic one-form basis and holomorphic one-form basis [15].*

2. *Compute holomorphic flow segmentation of the target surface, M^2, from the global conformal parameterization, ω^2, which conformally maps the 3D surface to a set of rectangles in the Euclidean plane.*

3. *Compute 2D conformal representation for the target surface, $\lambda^2(u, v)$ and $H^2(u, v)$, where (u, v) is the conformal coordinate;*

4. *Compute holomorphic flow segmentation of the source surface, M^1, and 2D conformal representation $\lambda^1(u, v)$ and $H^1(u, v)$;*

5. *Apply the mutual information method to optimize the correspondence between two surfaces, $t : (\lambda^1(u, v), H^1(u, v)) \rightarrow (\lambda^2(u, v), H^2(u, v)), j = 1, 2$ and $H^j(u, v), j = 1, 2$; and compute mutual information energy E_{MI}^0;*

6. *Compute derivative Dt.*

7. *Update the global conformal parameterization of source surface, M^1, by changing the coefficients $s^1(v) = Dt(v)\delta t$.*

8. *Compute mutual information energy E, with steps $3, 4, 5$.*

9. *If $E_{MI} - E_{MI}^0 < \delta E$, return t. Otherwise, assign E to E_0 and repeat steps 6 through 9.*

Currently, we use the following numerical scheme in step 6:

1. Compute dE_{MI}/du and dE_{MI}/dv, $du/ds_i, i = 1, 2, ..., 2g$;

2. Compute $dv/ds_i, i = 1, 2, ..., 2g$;

3. Compute $Dt = dE_{MI}/ds_i, i = 1, 2, ..., 2g$ with Equation 9.

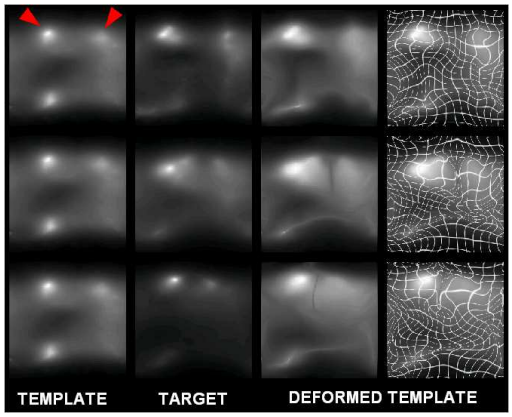

Figure 5. Matching surface features in 2D parameter domains using Mutual Information. Geometric features on 3D hippocampal surfaces (the conformal factor and mean curvature) were computed and compound scalar fields (e.g. 8xconformal factor + mean curvature) were mapped to a 2D square by conformal flattening. In the 2D parameter domain, data from a healthy normal subject (the template, leftmost column) was registered to data from several patients with Alzheimer's disease (target images, second column). Each mapping can be used to obtain a reparameterization of the 3D surface of the normal subject, by convecting the original 3D coordinates along with the flow. The deformed template images are shown in the third and fourth (gridded) columns. The grids show how the fluid transform expands some highly curved features to match similar features. Importantly, there are some consistent 3D geometric features that can be reidentified in the 2D parameter domain; e.g. bright areas (arrows) correspond to high curvature features in the head of the hippocampus.

4. Experimental Results

To make the results easier to illustrate, we chose to encode the profile of surface features using a compound scalar function $C(u,v) = 8\lambda(u,v) + H(u,v)$. We linearly normalized its dynamic range to the pixel intensity range 0 to 255. Several examples are shown, mapping one face to the other face and one hippocampal surface to another. Face mapping is useful for face recognition. The deformable surface registration of hippocampus is important for tracking developmental and degenerative changes in the hippocampus, as well as computing average shape models with appropriate boundary correspondences. Figure 5 shows the matching fields for several pairs of hippocampal surfaces, establishing correspondences between distinctive features. The velocity field v in Eqn 6 was computed iteratively by convolution of the force field with a filter kernel derived by Bro-Nielsen and Gramkow [4]. The viscosity coefficients λ and μ were set to 0.9 and 6.0 respectively. The deformation field in the parameter domain (u) was obtained from v by Euler integration over time, and the deformed template image was regridded when the Jacobian determinant of the deformation mapping at any point in $x - u$ was smaller than 0.5 [6]. At each step, the joint pdf was updated and the MI re-computed. Iterations were stopped when MI was no longer monotonically increasing or when the number of iterations reached 350. The Parzen parameter h was set to 10 for smoothing the joint pdf. In Figure 6, we show face surfaces and hippocampal surfaces to be matched, where the face surface was built with a high resolution, real-time 3D face acquisition system [31] and hippocampal surfaces were built from 3D MRI scans of the brain. Specifically, (a), (b) and (e), (f) show two surfaces to be matched; (c), (d) and (g) and (h) show 3D vector displacement map, connecting corresponding points on the two surfaces. (c) and (g) are before and (d) and (h) after reparameterization of the source surface using a fluid flow in the parameter domain. These more complex 3D vector fields store information on geometrical feature correspondences between the surfaces.

5. Conclusions and Future Work

We extended the mutual information method to match general surfaces. This is useful for face recognition and has numerous applications in medical imaging. Our examples of matching various hippocampal surfaces are relevant for mapping how degenerative diseases affect the brain, as well as building statistical shape models to detect the anatomical effects of disease, aging, or development. The face and hippocampus are used as specific examples, but the method is general and is applicable in principle to other surfaces.

Surface-based mutual information automates the matching of surfaces by computing a correspondence field guided by the joint distribution of features lying in both surfaces. This is a natural idea, in that it uses conformal parameterization to transform a surface matching problem into an image registration problem. Whether or not this approach provides a more relevant correspondences than those afforded by other criteria (minimum description length, neural nets, or hand landmarking) requires careful validation for each application. Optimal correspondence depends more on utility for a particular application than on anatomical homology. Because different correspondence principles produce different shape models, we plan to compare them in future for detecting group differences in brain structure, and individual differences in face recognition applications. . If statistical power is increased in group comparisons, this would support the use of correspondence fields established by mutual information on surfaces.

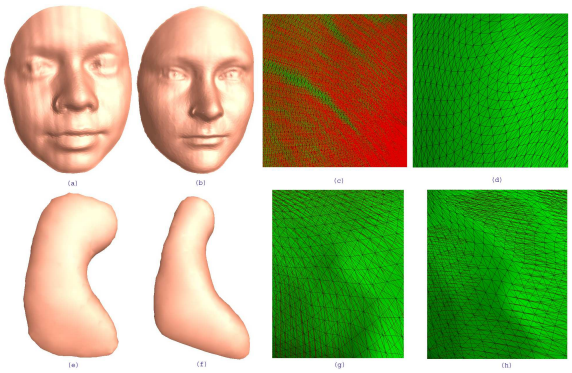

Figure 6. Surface matching results from our method. Panels (a), (b), (c) and (d) show the surfaces being matched. (a) and (b) are two face surfaces. (e) is a normal subject's hippocampal surface and (d) is an Alzheimer's disease patient's hippocampal surface. We flow the surface from (a) to (b) and from (e) to (f), respectively. Panels (c), (d), (g) and (h) show the 3D vector displacement map, connecting corresponding points on the two surfaces, (c) and (g) before and (d) and (h) after reparameterization of the source surface using a fluid flow in the parameter domain. After reparameterization, a leftward shift in the vertical isocurves adds a larger tangential component to the vector field. Even so, the deformed grid structure remains close to conformal. These more complex 3D vector fields store information on geometrical feature correspondences between the surfaces.

References

[1] S. Angenent, S. Haker, R. Kikinis, and A. Tannenbaum. Nondistorting flattening maps and the 3D visualization of colon CT images. *IEEE TMI*, 19:665–671, 2000.

[2] S. Angenent, S. Haker, A. Tannenbaum, and R. Kikinis. Conformal geometry and brain flattening. *MICCAI, Lecture Notes in Computer Science*, 1679:271–78, 1999.

[3] M. Bakircioglu, S. Joshi, and M. Miller. Landmark matching on brain surfaces via large deformation diffeomorphisms on the sphere. In *SPIE Medical Imaging*, volume 3661, pages 710–15, 1999.

[4] M. Bro-Nielsen and C. Gramkow. Fast fluid registration of medical images. In *Visualization in Biomedical Computing (VBC'96).*, volume 1131, pages 267–76. Springer, 1996.

[5] A. Bronstein, M. Bronstein, and R. Kimmel. Expression-invariant 3D face recognition. In *Proc. Audio & Video-based Biometric Person Authentication (AVBPA), Lecture Notes in Comp. Science*, volume 2688, pages 62–69. Springer, 2003.

[6] G. Christensen, R. Rabbitt, and M. Miller. Deformable templates using large deformation kinematics. *IEEE TIP*, 5(10):1435–47, 1996.

[7] J. Csernansky, S. Joshi, L. Wang, J. Haller, M. Gado, J. Miller, U. Grenander, and M. Miller. Hippocampal morphometry in schizophrenia via high dimensional brain mapping. *Proc. Natl. Acad. Sci.*, 95:11406–11, 1998.

[8] E. D'Agostino, F. Maes, D. Vandermeulen, and P. Suetens. A viscous fluid model for multimodal non-rigid image registration using mutual information. *Medical Image Analysis*, 7(4):565–75, 2003.

[9] C. Davatzikos. Spatial normalization of 3D brain images using deformable models. *J. Comp. Assisted Tomography*, 20(4):656–65, 1996.

[10] R. Davies, C. Twining, T. Cootes, J. Waterton, and C. Taylor. A minimum description length approach to statistical shape modeling. In *IEEE TMI*, volume 21, pages 525–37, 2002.

[11] B. Fischl, M. Sereno, R. Tootell, and A. Dale. High-resolution inter-subject averaging and a coordinate system for the cortical surface. In *Human Brain Mapping*, volume 8, pages 272–84, 1999.

[12] X. Gu and B. Vemuri. Matching 3D shapes using 2D conformal representations. In *MICCAI, Lectures Notes in Computer Science*, volume 3217, pages 771–80. Springer, 2004.

[13] X. Gu, Y. Wang, T. Chan, P. Thompson, and S.-T. Yau. Genus zero surface conformal mapping and its application to brain surface mapping. *IEEE TMI*, 23(8):949–58, Aug. 2004.

[14] X. Gu, Y. Wang, and S.-T. Yau. Geometric compression using Riemann surface. *Communication of Information and Systems*, 3(3):171–82, 2005.

[15] X. Gu and S.-T. Yau. Computing conformal structures of surfaces. *Communication of Information and Systems*, 2(2):121–46, 2002.

[16] G. Hermosillo. PhD thesis, Universitè de Nice (INRIA-ROBOTVIS), Sophia Antipolis, France, 2002.

[17] J. Huang, V. Blanz, and B. Heisele. Face recognition using component-based SVM classification and morphable models. In S.-W. Lee and A. Verri, editors, *SVM*, LNCS 2388, pages 334–41. Springer-Verlag, 2002.

[18] B. Kim, J. Boes, K. Frey, and C. Meyer. Mutual information for automated unwarping of rat brain autoradiographs. *NeuroImage*, 5(1):31–40, 1997.

[19] G. Kindlmann, D. Weinstein, A. Lee, A. Toga, and P. Thompson. Visualization of anatomic covariance tensor fields. In *Proc. IEEE EMBS*, San Francisco, CA, 2004.

[20] A. Leow, C. Yu, S. Lee, S. Huang, R. Nicolson, K. Hayashi, H. Protas, A. Toga, and P. Thompson. Brain structural mapping using a novel hybrid implicit/explicit framework based on the level-set method. *NeuroImage*, 24(3):910–27, 2005.

[21] N. Mavridis, F. Tsalakanidou, D. Pantazis, S. Malassiotis, and M. Strintzis. The HISCORE face recognition application: Affordable desktop face recognition based on a novel 3D camera. In *Proc. ICAV3D*, pages 157–60, 2001.

[22] C. Meyer, J. Boes, B. Kim, P. Bland, K. Zasadny, P. Kison, K. Koral, K. Frey, and R. Wahl. Demonstration of accuracy and clinical versality of mutual information for automatic multimodality image fusion using affine and thin plate spline warped geometric deformation. *Medical Image Analysis*, 1(3):195–206, 1997.

[23] E. Parzen. On the estimation of probability density function. *Annals of mathematical statistics*, 33:1065–76, 1962.

[24] A. Pentland. Looking at people: sensing for ubiquitous and wearable computing. *IEEE TPAMI*, 22(1):107–119, 2000.

[25] D. Rueckert, L. Sonoda, C. Hayes, D. Hill, M. Leach, and D. Hawkes. Nonrigid registration using free-form deformations: application to breast MR images. *IEEE TMI*, 18(8):712–21, 1999.

[26] P. Thompson, J. Giedd, R. Woods, D. MacDonald, A. Evans, and A. Toga. Growth patterns in the developing brain detected by using continuum-mechanical tensor maps. *Nature*, 404(6774):190–3, Mar. 2000.

[27] P. Thompson, R. Woods, M. Mega, and A. Toga. Mathematical/computational challenges in creating population-based brain atlases. In *Human Brain Mapping*, volume 9, pages 81–92, Feb. 2000.

[28] P. Viola and W. M. Wells. Alignment by maximization of mutual information. In *Proc. ICCV*, pages 16–23, Washington, DC, USA, 1995.

[29] W. Wells, P. Viola, H. Atsumi, S. Nakajima, and R. Kikinis. Multi-modal volume registration by maximization of mutual information. *Medical Image Analysis*, 1(1):35–51, 1996.

[30] J. West, J. Fitzpatrick, M. Wang, B. Dawant, C. Maurer, R. Kessler, R. Maciunas, C. Barillot, D. Lemoine, A. Collignon, F. Maes, P. Suetens, D. Vandermeulen, P. van den Elsen, S. Napel, T. Sumanaweera, B. Harkness, P. Hemler, D. Hill, D. Hawkes, C. Studholme, J. Maintz, M. Viergever, G. Malandain, X. Pennec, M. Noz, G. Maguire, M. Pollack, C. Pelizzari, R. Robb, D. Hanson, and R. Woods. Comparison and evaluation of retrospective intermodality brain image registration techniques. *J. Comp. Assisted Tomography*, 21(4):554–68, 1997.

[31] S. Zhang and P. Huang. High-resolution, real-time 3D shape acquisition. In *IEEE CVPR Workshop*, volume 3, page 28, Washington DC, USA, 2004.